

Effect of a driving electric field waveform on piezoelectric displacement of PZT thick films

Yuta KASHIWAGI,[†] Takashi IJIMA,* Takashi NAKAJIMA and Soichiro OKAMURA

Department of Applied Physics, Faculty of Science, Tokyo University of Science, 1–3 Kagurazaka, Shinjuku-ku, Tokyo 162–8601

*National Institute of Advanced Industrial Science and Technology, AIST Tsukuba West, 16–1 Onogawa, Tsukuba 305–8569

Endurance properties of piezoelectric-induced longitudinal displacement for lead zirconate titanate (PZT) thick films were investigated to develop microelectromechanical systems (MEMS). A 5- μm -thick film was prepared using chemical solution deposition (CSD). Square and triangle waveforms and various frequencies of unipolar or bipolar electric fields were applied to the film. The effects of applied field switching cycles on the ferroelectric properties and longitudinal displacements were measured using a twin-laser interferometer system. Under the bipolar applied field switching condition, the remanent polarization and piezoelectric displacement decreased concomitantly with increasing applied field switching cycles, similar to fatigue behavior. The applied field switching waveform and frequency affect the fatigue profile. The piezoelectric displacement did not decrease when the unipolar square and triangle waveform were applied to the samples. These results suggest that the unipolar driven PZT thick films are applicable to MEMS devices.

©2010 The Ceramic Society of Japan. All rights reserved.

Key-words : PZT, Thick film, Piezoelectric, Displacement, Fatigue

[Received April 22, 2010; Accepted July 15, 2010]

1. Introduction

In recent years, piezoelectric films have been well investigated for various applications such as sensors and actuators in microelectromechanical systems (MEMS).^{1)–3)} Miniaturization of MEMS devices is progressing using semiconductor fabrication techniques. For MEMS application, the $\text{Pb}(\text{Zr,Ti})\text{O}_3$ (PZT) is considered the most promising material because of its superior piezoelectric and ferroelectric properties. To realize MEMS devices with piezoelectric films, it is necessary to achieve sufficient piezoelectric longitudinal displacement. One way to take large displacement is to increase the film thickness. For MEMS devices, the piezoelectric film thickness must usually be greater than 1 μm . We can prepare PZT films with thickness of about 10 μm using progressive chemical solution deposition (CSD).⁴⁾ Another way to achieve large displacement—a high drive electric field higher than the coercive field (E_c)—is applied to the piezoelectric films. For bulk piezoelectric ceramics devices, the driving electric field is less than E_c . Therefore, the driving electric field condition of the films differs from that of the bulk ceramics. The effects of the applied field switching cycles on the ferroelectric properties of the thin films with thickness less than 1 μm have been well investigated for ferroelectric random access memory (FeRAM) applications.^{5),6)} However, detailed piezoelectric thick film characteristics for the relation between the longitudinal displacement and applied field switching condition have not been well investigated. It is important to clarify the longitudinal displacement endurance properties of the thick piezoelectric films driven with the high electric field to develop actual piezo-MEMS devices. As described in this paper, we investigated the endurance of PZT thick films applied with various field switching conditions such as polarity, waveforms, and frequency.

2. Experimental procedure

First, a $\text{Pb}(\text{Zr,Ti})\text{O}_3$ (Zr:Ti = 53:47) thick film was deposited on Pt/Ti/SiO₂/Si substrate using CSD. The film thickness was 5 μm . After deposition, a 200-nm-thick Pt top electrode was deposited by sputtering. Then a column-shaped capacitor with 200 μm diameter was fabricated using photolithography. Details of the fabrication process were described elsewhere.⁴⁾ To measure the piezoelectric induced longitudinal displacement of the PZT films, a twin-laser displacement measurement system was used. This system had two individual laser interferometers to subtract the effect of substrate bending from the longitudinal displacement. A topside laser interferometer (MLD-102; NEOARK) measures the top electrode displacement. The bottom side laser interferometer (MLD-301A; NEOARK) measures the silicon substrate displacement. Two interferometers were connected with the ferroelectric test system (FCE-1; Toyo Corp.). The detail of the sample measurement configuration is exhibited in **Fig. 1**. The FCE drive terminal (positive) was connected to the top electrode, and the return terminal (negative) was connected to the bottom electrode. The voltage was applied in the positive direction, “+” was applied to the top electrode. This system can measure the longitudinal displacement and the polarization hysteresis loop of the PZT films simultaneously.

A bipolar or unipolar applied field of a triangle waveform was used to measure the ferroelectric properties and longitudinal displacement. The measurement frequency was 100 Hz, and the amplitude of the applied fields was $\pm 80 \text{ kV/cm}$ (40 V) for bipolar, and 80 kV/cm (40 V) for unipolar fields that were four times higher than coercive fields of the prepared PZT film samples: $E_c = 20 \text{ kV/cm}$. From the measured piezoelectric longitudinal displacement, the difference between the maximum displacement and the center of the butterfly curve (cross point) was defined as $\pm d_{\text{max}}$ for bipolar measurement. The difference between maximum displacement and the displacement at 0 V was defined as d_{max} in the case of unipolar measurement. To evaluate

[†] Corresponding author: Y. Kashiwagi; E-mail: yuta-kashiwagi@aist.go.jp

the endurance properties, a switching electric field of bipolar or unipolar was applied to the film samples. After several switching cycles, the ferroelectric properties and longitudinal displacement were measured. The waveforms of the switching field for endurance evaluation were square and triangular; the frequency was changed from 100 kHz to 100 Hz. The amplitude of the applied switching field was ± 80 kV/cm for bipolar, and 80 kV/cm for the unipolar. Details of the measurement setting, the definition of d_{\max} , and switching field setting are presented in Fig. 2.

3. Results and discussion

3.1 Endurance evaluation of bipolar electric field switching

Figure 3(a) shows the ferroelectric response (P - E hysteresis loop); Fig. 3(b) shows the piezoelectric longitudinal displacement response (butterfly curve) before and after 10^6 cycles of triangle bipolar field switching at 100 Hz. There is correlation between P - E hysteresis loop and butterfly curve before switching, generally, because coercive fields, $\pm E_c$, at positive and negative applied field in Fig. 3(a) correspond to applied fields at minimum displacement in Fig. 3(b). It is apparent that the remanent polarization, P_r , decreases after 10^6 cycles of field switching, and that E_c shifts to the negative field direction in Fig. 3(a). That this P_r behavior decreases with applied field switching cycles is described as the polarization fatigue phenomenon of PZT thin films.⁶⁾⁻⁸⁾ In Fig. 3(b), piezoelectric

longitudinal displacement showed an asymmetric shape after 10^6 cycles of field switching. Moreover, the minimum displacement corresponding $\pm E_c$ shifts to the negative direction like the fatigued P - E hysteresis loop in Fig. 3(a). The maximum displacement of the negative field ($-d_{\max}$) decreased, but that of the positive field ($+d_{\max}$) showed no remarkable difference. The reason of this asymmetry seems to be the shift of E_c like imprint.⁹⁾ This asymmetry of the displacement after bipolar field switching cycles is consistent with results described in other reports of piezoelectric fatigue studies.^{10),11)}

Figure 4 presents the relation between the applied field switching cycles and the normalized remanent polarization, P_r/P_{r0} , which is switched remanent polarization/initial remanent polarization, for (a) a square-wave bipolar field and (b) a triangle-wave bipolar field. For both waveforms, P_r/P_{r0} decreased and recovered with increasing switching cycles, as reported else-

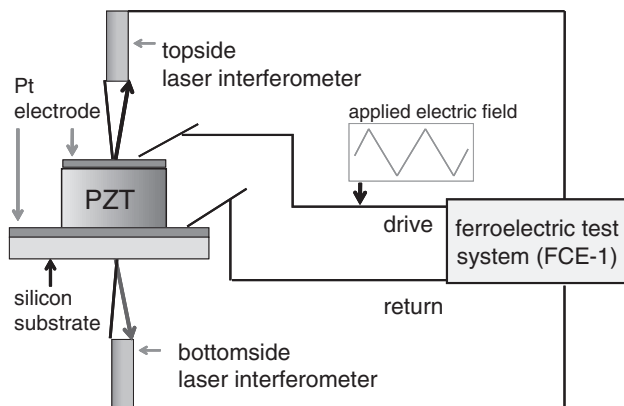


Fig. 1. Detailed sample measurement configuration.

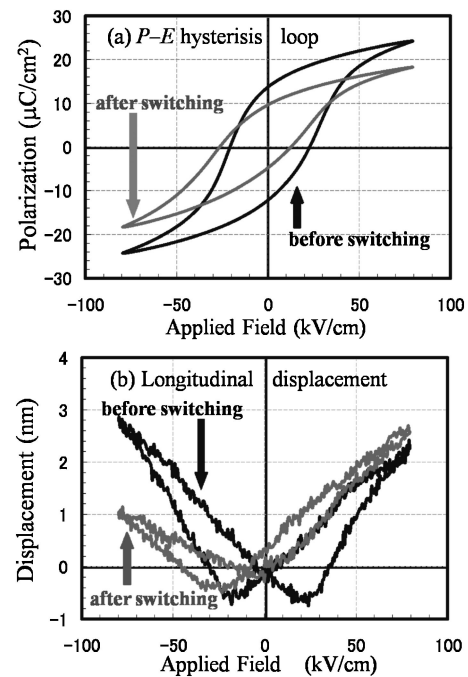


Fig. 3. Ferroelectric and piezoelectric responses before and after applied field switching cycles of triangle wave: (a) P - E Hysteresis loop (b) Butterfly curve.

	Measurement Sequence	Definition of d_{\max}	Endurance Sequence	
Bipolar Setting			Square waveform	Triangle waveform
Unipolar Setting			Square waveform	Triangle waveform

Fig. 2. Detailed measurement settings and the definition of d_{\max} ; switching field settings for endurance evaluation.

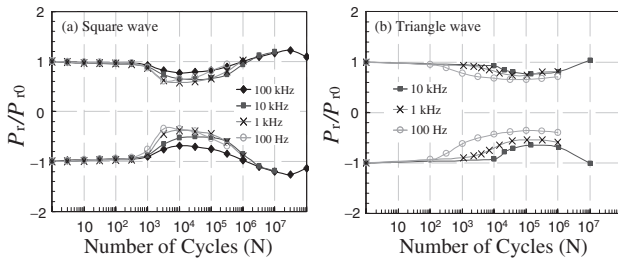


Fig. 4. Switching cycle dependence on normalized remanent polarization for (a) a square-wave bipolar field and (b) triangle-wave bipolar field.

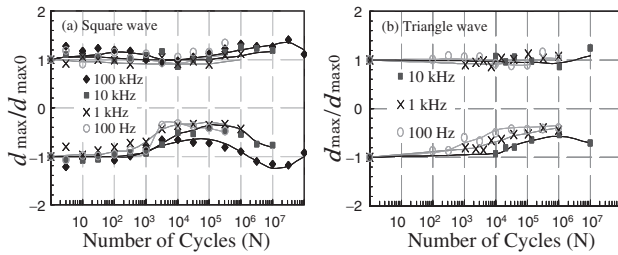


Fig. 5. Switching cycle dependence on normalized piezoelectric displacement for (a) a square-wave bipolar field and (b) triangle-wave bipolar field.

where.¹²⁾ For the square-wave bipolar field depicted in Fig. 4(a), degradation of P_r/P_{r0} started at 10^3 cycles. The degradation rate increased concomitantly with decreasing square-wave frequency. On the other hand, when the triangle-wave bipolar field was applied as depicted in Fig. 4(b), onset cycles of the degradation increased from 10^2 to 10^4 with increasing switching frequency from 100 Hz to 10 kHz. The degradation rate increased concomitantly with decreasing triangle-wave frequency. Based on these results, the waveform and wave frequency of the applied bipolar field are considered to affect the onset cycles of the fatigue and fatigue rate.

Figure 5 presents the relation between the bipolar field switching cycles and normalized bipolar longitudinal displacement of the sample ($d_{\max}/d_{\max0}$) for (a) a square-wave bipolar field and (b) a triangle-wave bipolar field. It is apparent that the normalized displacement in the negative electric field decreased concomitantly with increasing switching cycles such as polarization fatigue, as depicted in Fig. 4. The fatigued profile of the displacement is similar to the pattern of polarization, which means that the effect of the applied waveform and the applied frequency on the onset cycles of the displacement degradation and the displacement degradation rate show the same tendency for polarization. In contrast, the normalized displacement in a positive field showed no degradation. The applied waveform and the applied frequency did not affect the displacement, as presented in Fig. 3.

Figure 6(a) shows the relation between the minimum value of the normalized remanent polarization and the applied field switching frequency. The minimum values of normalized remanent polarization of positive ($+P_r/P_{r0}$) and negative ($-P_r/P_{r0}$) field decreased concomitantly with decreasing applied field frequency. Moreover, for a triangle waveform, the amount of fatigued polarization was slightly larger than in the case of a square waveform. This waveform dependency of the PZT thin film was reported.¹³⁾ The values for the square waveform are $+P_r/P_{r0} = 0.66$ and $-P_r/P_{r0} = 0.52$ at 10 kHz; the values are

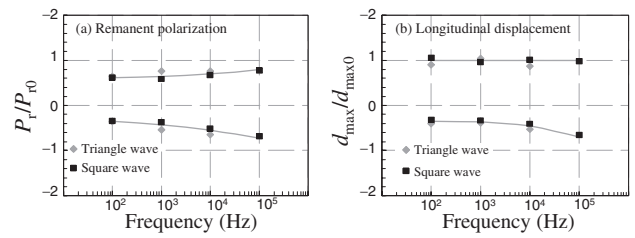


Fig. 6. (a) Relation between the minimum value of the normalized remanent polarization and the applied field switching frequency. (b) Relation between the minimum value of the normalized displacement and the applied field switching frequency.

$+P_r/P_{r0} = 0.61$ and $-P_r/P_{r0} = 0.34$ at 100 Hz. The values for a triangle waveform are $+P_r/P_{r0} = 0.76$. They are $-P_r/P_{r0} = 0.65$ at 10 kHz and $+P_r/P_{r0} = 0.65$ and $-P_r/P_{r0} = 0.36$ at 100 Hz. These results suggest that the effective time of applied electric field, as estimated from parameters such as the waveform, number of switching cycles N and frequency f , affects the fatigue behavior of polarization.^{14),15)}

Figure 6(b) shows the relation between the minimum value of the normalized displacement and the applied field switching frequency. The minimum value of the normalized displacement of the negative field ($-d_{\max}/d_{\max0}$) decreased concomitantly with decreasing applied pulse frequency like $-P_r/P_{r0}$ in Fig. 6(a), although the minimum value of the normalized displacement of the positive field ($+d_{\max}/d_{\max0}$) did not decrease, as portrayed in Fig. 5. To date, the reason for the asymmetric displacement behavior remains unclear. However, the reason for asymmetric displacement behavior is assumed to be the biased electric field induced by space charge accumulation¹⁰⁾ or the asymmetric pinning of domain walls.¹¹⁾ Therefore, the increase of pinned non-180-degree domain area is suspected as the reason, but further experiments must be undertaken to clarify this phenomenon.

3.2 Endurance evaluation of unipolar electric field switching

Figures 7(a)–7(d) portray the relation between the various frequencies of unipolar field switching cycles and normalized unipolar longitudinal displacement ($d_{\max}/d_{\max0}$). Apparently, the normalized unipolar longitudinal displacement showed no degradation with increasing positive unipolar field switching cycles. This tendency did not change when the applied field frequency was changed from 100 Hz to 100 kHz for square and triangle waveforms. Therefore, the longitudinal piezoelectric displacement showed no fatigue behavior under the positive unipolar field switching at the presented measurement configuration. After the 10^8 cycles of 100 kHz square unipolar field applied to the film as shown in Fig. 7(d), the bipolar measurement of the ferroelectric and piezoelectric displacement properties was performed. The P - E hysteresis loops did not show distinguished change between before and after unipolar field switching, and longitudinal piezoelectric displacement also did not show distinguished change. This behavior is different from that of bipolar field switching as shown in Fig. 3. Moreover, in the cases of 100 Hz triangle, 10 kHz square, 100 kHz triangle unipolar field, the unipolar longitudinal displacement increased concomitantly with increasing the applied field switching cycles. This evolution of unipolar longitudinal displacement was attributed to reorientation of the non 180-degree domain of the prepared PZT films. This

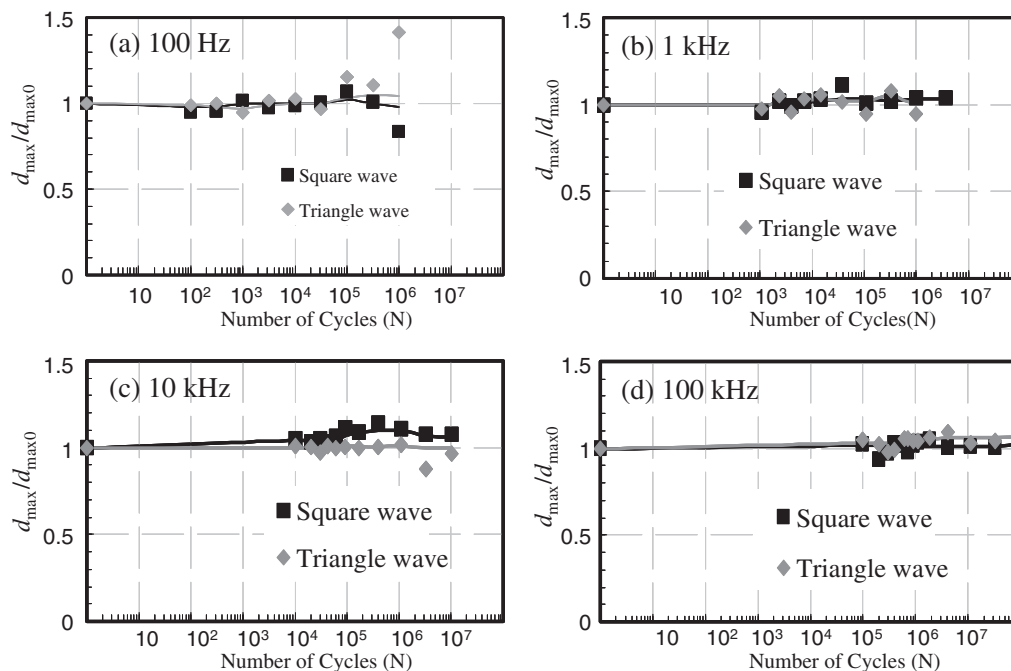


Fig. 7. Relation between the various frequencies of unipolar field switching cycles and the normalized unipolar longitudinal displacement ($d_{\max}/d_{\max0}$): (a) 100 Hz, (b) 1 kHz, (c) 10 kHz, and (d) 100 kHz.

mechanism is consistent with the pulse poling process described elsewhere.¹⁶⁾ Therefore, the relation between unipolar field switching cycle and the effect of the poling process should be investigated in future studies.

4. Conclusion

Various waveforms and frequency of unipolar or bipolar electric field were applied to 5- μm -thick PZT films. Under the bipolar applied electric field condition, the remanent polarization and piezoelectric displacement decreased concomitantly with increasing field switching cycles as in fatigue behavior. The applied field waveform and frequency affect the onset of polarization fatigue and fatigue rate. However, a difference was found between the degradation of polarization and piezoelectric displacement. The reason underlying the asymmetric displacement fatigue behavior is expected to be the effect of pinned non-180-degree domains, but further investigations must be undertaken to clarify this point. Under the positive unipolar applied electric field condition at the presented measurement configuration, the piezoelectric displacement did not decrease for the square and triangle waveforms. These results suggest that the PZT thick films for MEMS applications have good endurance property under a unipolar electrical field condition. However, in several unipolar field switching conditions, the unipolar longitudinal displacement increased concomitantly with increasing cycle application because of the pulse poling effect. Therefore, the relation between the unipolar field switching cycle and poling process effects should be investigated in future studies.

References

- 1) S. T. McKinstry and P. Muralt, *J. Electroceram.*, **12**, 7–13 (2004).
- 2) P. Gerber, A. Roelofs, C. K  gler, U. B  ttger, R. Waser and K. Prume, *J. Appl. Phys.*, **96**, 2800–2804 (2004).
- 3) T. Yamamoto, M. Yamamoto, K. Nishida, H. Funakubo, T. Iijima, T. Aiso and Y. Ichikawa, *Jpn. J. Appl. Phys.*, **48**, 09KA04 (2009).
- 4) T. Iijima, S. Osone, Y. Shimoojo and H. Nagai, *Int. J. Appl. Ceram. Technol.*, **3**, 442–447 (2006).
- 5) J. F. Scott and C. A. Araujo, *Science*, **246**, 1400–1405 (1989).
- 6) K. Lee, B. R. Rhee and C. Lee, *Appl. Phys. Lett.*, **79**, 821–823 (2001).
- 7) A. K. Tagantsev, I. Stolichnov, E. L. Colla and N. Setter, *J. Appl. Phys.*, **90**, 1387–1402 (2001).
- 8) E. L. Colla, D. V. Taylor, A. K. Tagantsev and N. Setter, *Appl. Phys. Lett.*, **72**, 2478–2480 (1998).
- 9) A. Gruverman, O. Auciello and H. Tokumoto, *Appl. Phys. Lett.*, **69**, 3191–3193 (1996).
- 10) D. Ricinchi and M. Okuyama, *Appl. Phys. Lett.*, **81**, 4040–4042 (2002).
- 11) A. L. Kholkin, E. L. Colla, A. K. Tagantsev, D. V. Taylor and N. Setter, *Appl. Phys. Lett.*, **68**, 2577–2579 (1996).
- 12) G. Le Rhun, G. Poullain, R. Bouregba and G. Leclerc, *J. Eur. Ceram. Soc.*, **25**, 2281–2284 (2005).
- 13) G. Le Rhun, G. Poullain and R. Bouregba, *J. Appl. Phys.*, **96**, 3876–3880 (2004).
- 14) S. B. Majumder, Y. N. Mohapatra and D. C. Agrawal, *Appl. Phys. Lett.*, **70**, 138–140 (1997).
- 15) G. Zhu, Z. Zeng, L. Zhang and X. Yan, *Appl. Phys. Lett.*, **89**, 102905 (2006).
- 16) M. Kohli, P. Muralt and N. Setter, *Appl. Phys. Lett.*, **72**, 3217–3219 (1998).